1st International Workshop on High-Order CFD methods
High-Order Accurate Numerical Solutions for
Unsteady Viscous Flow over Tandem Airfoils

by

Konstantinos Kontzialis
kontzialis@iacm.forth.gr

and

John A. Ekaterinaris
ekaterin@iacm.forth.gr

School of Mechanical and Aerospace Engineering
University of Patras, Greece

1. Code description

Numerical solutions for the two-dimensional, compressible Navier-Stokes equations are obtained using ***HoAc*** (High order Accuracy), a CFD solver based on the discontinuous Galerking (DG) finite element method. Explicit or implicit Runge-Kutta time marching methods can be used for time accurate numerical solutions. Arbitrary high order, tensor product orthogonal Jacobi polynomial bases are formed for the standard square element of the reference space and mapped to the physical domain elements through collapsed coordinate transformations. High order accurate discretizations can be obtained for mixed-type meshes, and p-adaptive capabilities exist. The code is fully parallelized for both explicit and implicit time marching schemes using PETSc. Post processing of the results is performed with Paraview using a high order discontinuous output.

2. Case summary

In all the simulations regarding the sensitivity study for the distance of far field boundary, a P2 (third order accurate) expansion at every element was employed. For the time accurate simulations a P2, P3, and P4 expansion was employed on a mesh with refined elements in the vicinity of the airfoils. The airfoils were assumed to correspond to an adiabatic wall. The initial conditions correspond to that for case A. In all the simulations straight sided elements have been used.

3. Mesh

The far filed boundary was presented by a circle. A rectangle of size 5x2 was constructed around the airfoils and a hybrid mesh with quadrilateral elements for the near wall flow region and triangles for the rest of the domain was generated with straight sided elements, in order to keep the same mesh resolution in the vicinity of the airfoils for varying distance of the far field boundary. The mesh in the rectangular region is depicted in Fig. 1.

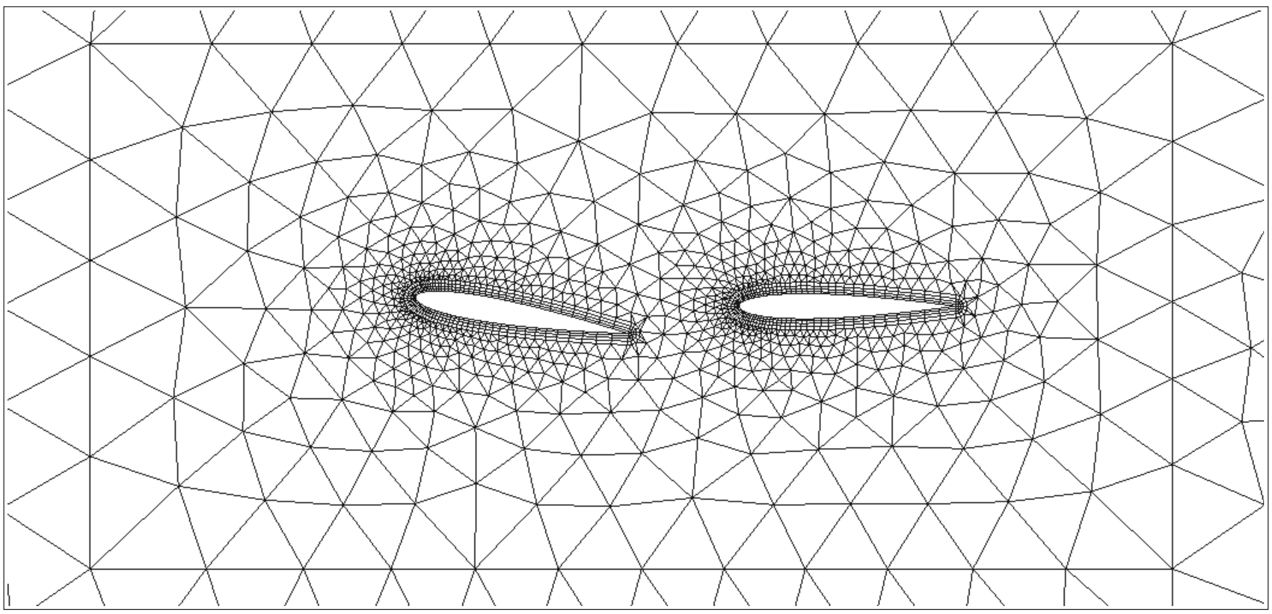

Fig. 1 Hybrid mesh in the vicinity of the airfoils for the sensitivity study on the far field distance.

4. Results for requirement 1

The far field boundary was formed by a circle enclosing the airfoils. Three simulations were performed in order to examine the effect of the far field boundary distance from the airfoils. These corresponded to the following radii of the circles: R=25, R=50, R=100 times the chord length of the airfoil, which was assumed equal to unity. The sensitivity study was performed using an explicit third order RK SSP scheme with 16 stages up to T = 100, using a time step size of **dt = 5.0e-4**, corresponding to non-dimensional units.

In Table 1 the work units, number of elements, number of DOF and the L_2 error for the whole time of the simulation for the aerodynamic coefficients for both airfoils are given. All the simulations were performed using 8 processors. From the results given in Table 1, the distance of the far field for the time accurate simulations was chosen to be R=50.

R	# Elem.	Work units	nDOFs	Error C_l Forward Airfoil	Error C_d Forward Airfoil	Error C_l Aft Airfoil	Error C_d Aft Airfoil
25	2708	1163.49	146496	--	--	--	--
50	2788	1312.3	150336	5.4880e-7	1.0240e-7	2.1443e-6	1.6780e-7
100	2914	1649.78	156384	6.8725e-8	1.0516e-8	1.2230e-7	3.0579e-8

Table 1. Work units and error in aerodynamic coefficients for the effect of the far field distance from the airfoils using an explicit third order SSP method.

5. Results for requirement 2

In the present work the order of approximation on the results produced by the simulations was examined. A finer mesh in the vicinity of the airfoils (Fig. 2), with 5650 elements in total, was generated.

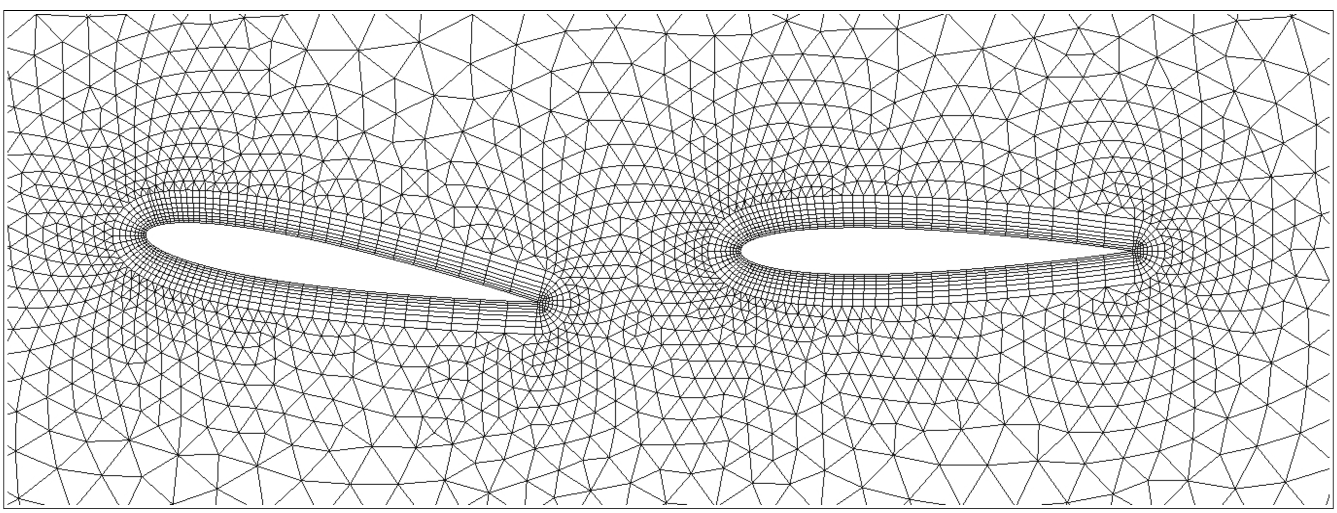

Fig. 2 Hybrid mesh in the vicinity of the airfoils used for time accurate computations.

Three simulations were performed with a P2, P3 and a P4 expansion using an explicit third order SSP Runge- Kutta method with 16 stages and a time step of **dt = 1.0e-3** corresponding to non-dimensional units. The mesh is depicted in Fig. 2. The airfoils were discretized using 80 elements. The minimum element length on the airfoils is equal to 4.52e-3, starting from the leading edge and the maximum element length is equal to 7.33e-2 at the trailing edge. The simulations were performed using 16 processors.

In Table 2, the number of DOF, work units and the L_2 error in the computation of the aerodynamic coefficients are given for each order of approximation.

Order	nDOF	Work Units	**Error C_l Forward Airfoil**	**Error C_d Forward Airfoil**	**Error C_l Aft Airfoil**	**Error C_d Aft Airfoil**
P2	16195.2	787.54	--	--	--	--
P3	37999.6	1847.84	0.023	0.0273	1.3043	0.1052
P4	120038	5837.2	1.0654e-04	1.3222e-05	5.2453e-04	4.6965e-05

Table 2. Work units for time accuracy study.

From Table 2 it is observed that the results from the P4 computation are close to the requirements of the case.

In Figs. 3 and 4 the time history profile of the aerodynamic coefficients for the forward airfoil obtained from the P2, P3 and P4 computations are depicted:

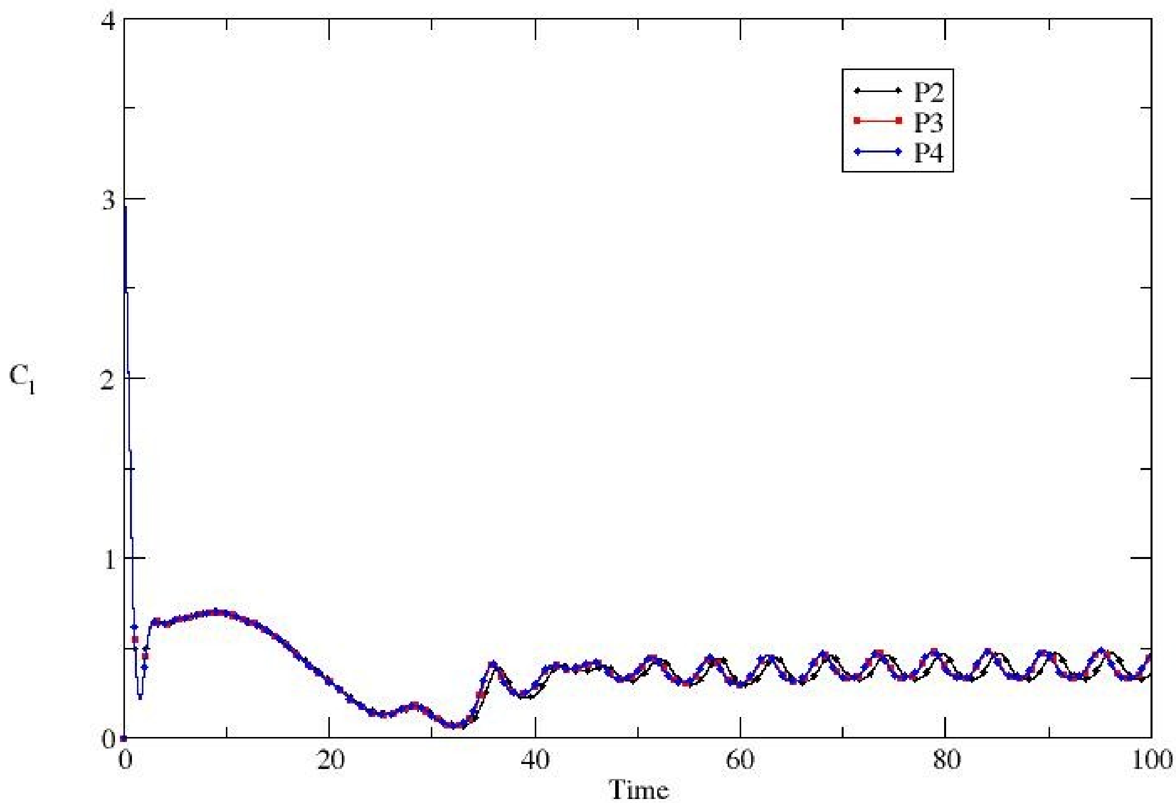

Fig. 3 Time history of the lift coefficient C_l for the forward airfoil.

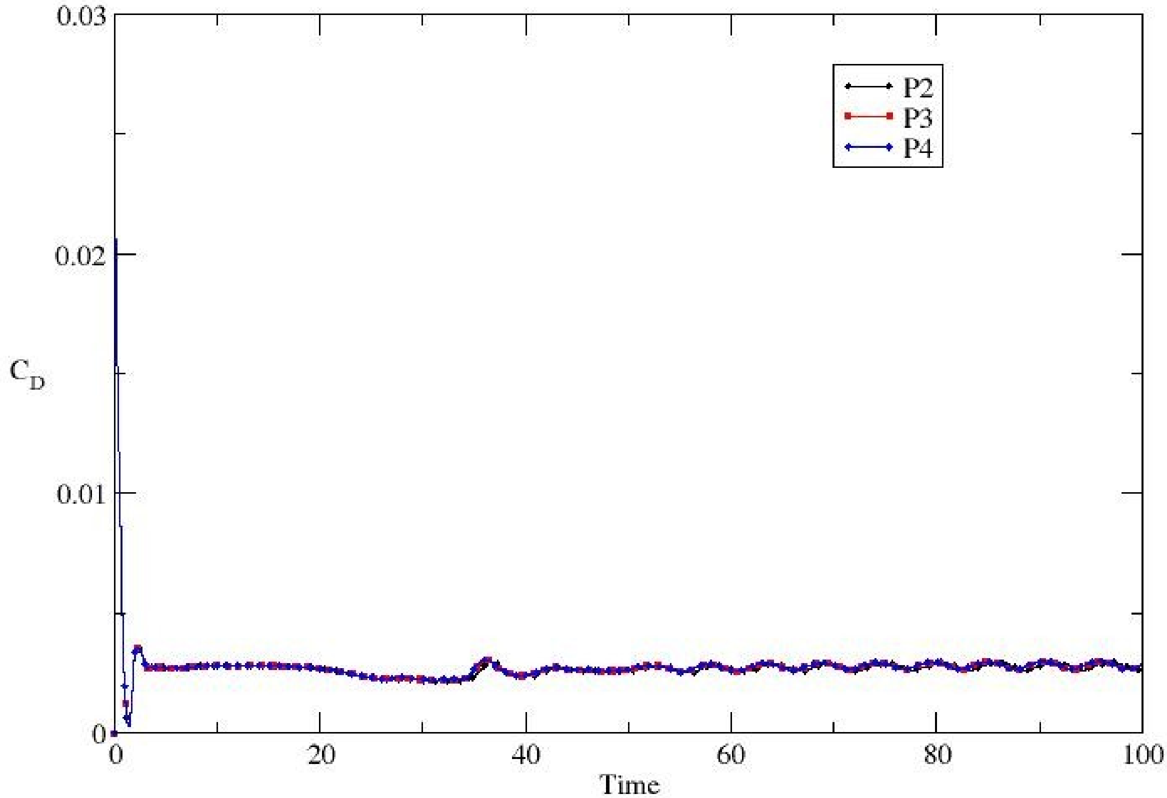

Fig. 4 Time history of the drag coefficient C_D for the forward airfoil.

In Figs. 5 and 6 the time history profile of the aerodynamic coefficients for the aft airfoil obtained from the P2, P3 and P4 computations are depicted:

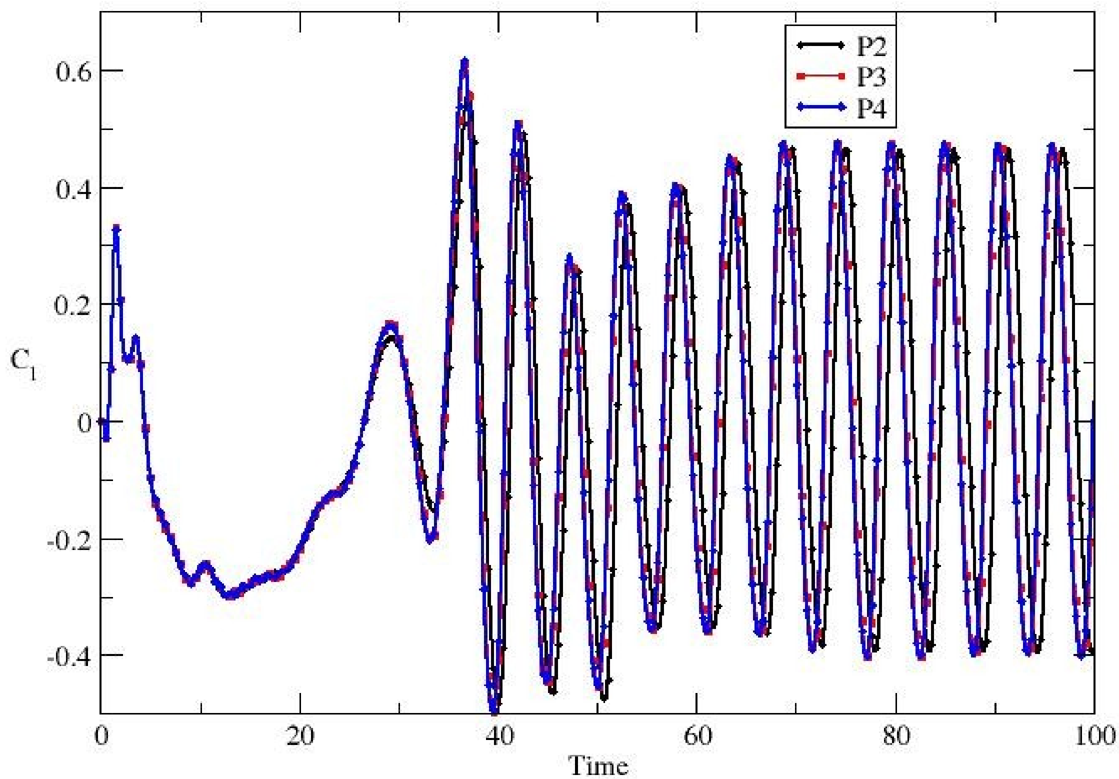

Fig. 5 Time history of the lift coefficient C_l for the aft airfoil.

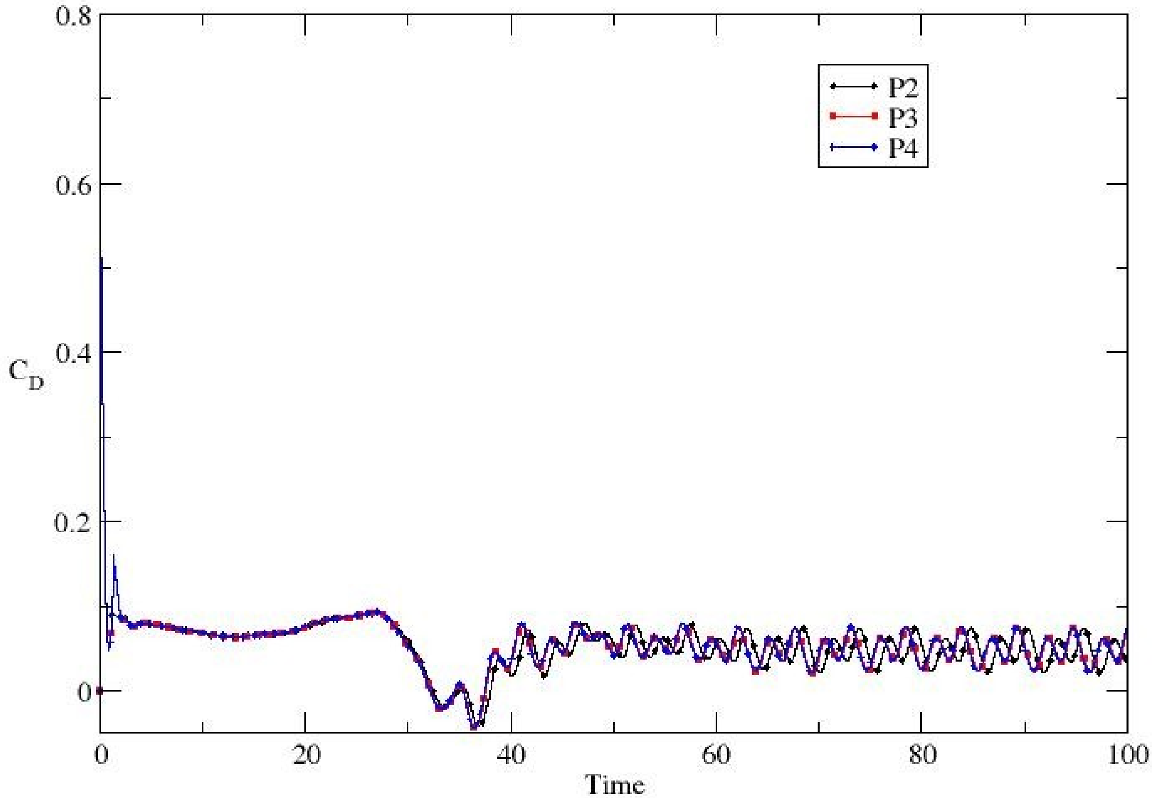

Fig. 6 Time history of the drag coefficient C_D for the aft airfoil.